Polymer Chemistry

Accepted Manuscript

This is an *Accepted Manuscript*, which has been through the Royal Society of Chemistry peer review process and has been accepted for publication.

Accepted Manuscripts are published online shortly after acceptance, before technical editing, formatting and proof reading. Using this free service, authors can make their results available to the community, in citable form, before we publish the edited article. We will replace this *Accepted Manuscript* with the edited and formatted *Advance Article* as soon as it is available.

You can find more information about *Accepted Manuscripts* in the Information for Authors.

Please note that technical editing may introduce minor changes to the text and/or graphics, which may alter content. The journal's standard Terms & Conditions and the Ethical guidelines still apply. In no event shall the Royal Society of Chemistry be held responsible for any errors or omissions in this *Accepted Manuscript* or any consequences arising from the use of any information it contains.

ROYAL SOCIETY OF CHEMISTRY

www.rsc.org/polymers

Cite this: DOI: 10.1039/c0xx00000x

www.rsc.org/xxxxxx

Article

Facile Synthesis of Multifunctional Copolymer via a Concurrent RAFT-Enzymatic System for Theranostic Applications

Changkui Fu[1], Andre Bongers[2], Ke Wang[1], Bin Yang[1], Yuan Zhao[1], Haibo Wu[1,4], Yen Wei[1], Hien T. T. Duong[3]*, Zhiming Wang[4]*, Lei Tao[1]*

Received (in XXX, XXX) Xth XXXXXXXXX 20XX, Accepted Xth XXXXXXXXX 20XX
DOI: 10.1039/b000000x

Facile preparation of well-defined and multifunctional polymers is of great importance for the development of polymer-based drug carriers. By performing enzymatic transacylation during RAFT polymerization, diverse monomers with different functions were generated *in situ* and simultaneously copolymerized via the RAFT process to form a well-defined multifunctional copolymer precursor which contains fluorine, polyethylene glycol (PEG), benzaldehyde and azido groups. The glucose moiety (which represents a possible targeting group for tumor treatment) was conjugated to this precursor via a copper-catalyzed azide alkyne cycloaddition (CuAAc) reaction to generate the polymer drug carrier. A ^{19}F MRI phantom was performed for the polymer drug carrier, indicating its potential as a possible ^{19}F MRI tracer. The polymer drug carrier has been shown to specifically bind to lectin due to the contained glucose moiety, demonstrating its potential targeting effect. Then, doxorubicin (dox, an anticancer drug) was conjugated with the polymer drug carrier through imine chemistry to generate target polymer-dox complex. This polymer-dox complex possesses amphiphilic character so self-assembles in aqueous solution into spherical micelles with size of ~30 nm, which exhibit much faster release of dox at pH 5.5 than at pH 7.4. Subsequent cell experiments showed the polymer-dox complex is less toxic than native dox to normal cells while retaining similar cytotoxicity against cancer cells, suggesting the polymer drug carrier is potentially a safe and effective drug delivery system. We believe that as several reactive moieties can be implanted into the polymer structure in a one-pot manner to achieve a multifunctional polymer precursor for efficient post-modification, this concurrent tandem polymerization (CTP) system might be useful for the development of novel anticancer theranostic nanomedicines.

Introduction

Theranostic nanomedicine has drawn much attention due to its capacity for simultaneous disease diagnosis and therapy.[1-3] Theranostic nanomedicine integrates therapeutic agents and molecular-level tracking agents, bridging the gap between therapy and imaging to facilitate real-time monitoring the efficacy of clinical treatment.[4-7] A variety of treatments based on inorganic materials including gold nanoparticles,[8,9] silica nanoparticles,[10,11] semiconductor quantum dots[12,13] and superparamagnetic iron oxide nanoparticles[14-16] have been developed and achieved significant academic acclaim. However to date they haven't been widely used in clinical applications due to uncertainties around long-term safety.[17-19] By contrast, polymeric materials can be designed with excellent biocompatibility, biodegradability, and structural versatility and hence represent attractive potential candidates for theranostic applications.[20-28] The fabrication of polymeric theranostic nanomedicine involves synthesis of multifunctional polymers integrating imaging, therapeutic and targeting functional groups.[29-31] Among those polymeric theranostic nanomedicines, glycopolymer-based theranostic materials show distinct advantages in tumor diagnosis and therapy due to the intrinsic biocompatibility and targetability of glycopolymers.[32] Typically, such multifunctional polymers are obtained through polymerization of several functional monomers previously synthesized via multiple organic reactions requiring laborious and time consuming operations such as the separation and purification of intermediates and target precursors. This complexity has become the main hurdle to impede further research. In this regard, developing facile strategies is significant for both fundamental research and practical applications.

Concurrent tandem polymerization (CTP) is a new polymerization methodology based on the controlled radical polymerization method (CRP) in which orthogonal organic reactions for monomer synthesis or end group modification can be simultaneously performed with CRP such as atom transfer radical polymerization (ATRP) or reversible addition-fragmentation chain transfer (RAFT) polymerization.[33-38] CTP integrates the process of monomer synthesis/end group modification and polymerization in one pot, providing a simple and versatile method for the synthesis of polymers with specific functional side/end groups. Our group has developed several CTP systems by introducing enzymatic transacylation to CRP (ATRP or RAFT).[35,39-42] The enzymatic transacylation between active acyl donor trifluoroethyl methacrylate (TFEMA) and an alcohol (ROH) occurred efficiently and led to *in situ* monomer

transformation from TFEMA to the target alcohol-based methacrylate monomer (RMA), which instantly took part in the CRP process to generate the final polymer. Since the concurrent CRP-enzymatic multicomponent polymerization system avoids the laborious synthesis and purification of corresponding monomers, it might be a suitable candidate for the facile synthesis of multifunctional copolymers.

Herein, using this CRP-enzymatic system we have prepared multifunctional copolymers containing different functionalities. As shown in Scheme 1a, enzymatic transacylation of TFEMA and three functional alcohols: 3-azido propanol (AP), 4-((6-hydroxyhexyl)oxy)benzaldehyde (HBA), and methoxypolyethylene glycol (mPEG, M_n ~ 350) were combined with RAFT polymerization in one pot where the enzymatic transacylation *in situ* generated three functional monomers based on the corresponding alcohols. As expected, the final polymer contained up to four functional groups (three alcohols plus fluoride residue) and was able to be used as the precursor for the fabrication of multifunctional theranostic polymeric nanomedicines.

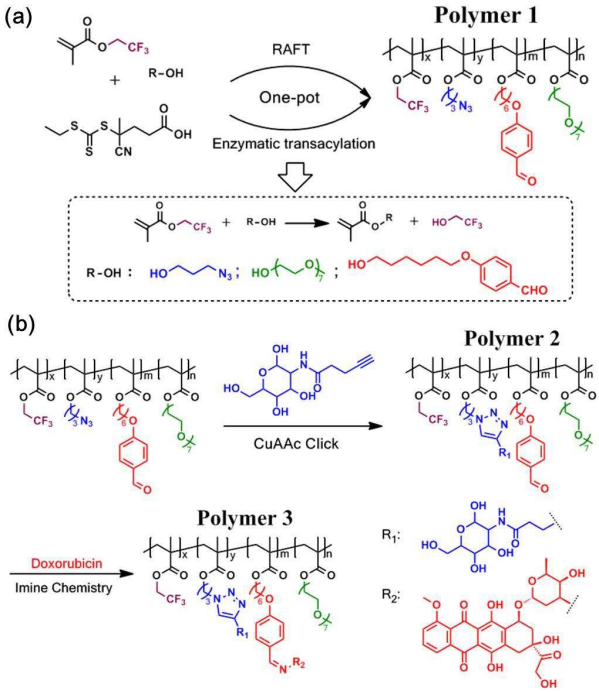

Scheme 1 (a) One-pot synthesis of multifunctional copolymer (**Polymer 1**) via concurrent RAFT polymerization and enzymatic monomer transformation; (b) post-modification of multifunctional copolymer via sequential CuAAc click reaction and imine chemistry to introduce glucose (**Polymer 2**) and dox (**Polymer 3**).

As illustrated in Scheme 1b: 1) the fluorinated residue can be used as the contrast agent for ^{19}F MRI; 2) the azido group can be simply modified via the efficient copper-catalyzed azide alkyne cycloaddition (CuAAc) click reaction to introduce glucose moiety as the potential targeting group; 3) the aldehyde group can be employed to link amine contained drugs such as dox; 4) the PEG segment can greatly promote the water solubility and biocompatibility of polymeric nanomedicine. These properties make the polymer ideal for theranostic applications as it integrates several functionalities including capabilities as a ^{19}F MRI tracking agent, anti-cancer drug, targeting moiety and biocompatibility. Compared with conventional methods, the current CTP system avoids the multi-step synthesis of various functional monomers in multifunctional copolymer synthesis, and saves time and resources. By introducing intact reactive modules into the polymer structure and utilizing highly efficient coupling reactions to modify the precursor following polymerization, we potentially create a simply-prepared theranostic agent, suggesting a possible new approach to multifunctional theranostic polymeric materials.

Results and discussions

RAFT polymerization in the presence of concurrent enzymatic monomer transformation has been employed to synthesize **Polymer 1** (Scheme 1) using the 4-cyano-4-(ethylthiocarbonothioylthio) pentanoic acid (CETPA) and 2,2'-azobis-(2,4-dimethylvaleronitrile) (ABVN) as the chain transfer agent (CTA) and initiator, respectively. The polymerization was conducted at 50 °C in toluene and the initial feeding ratio of [CTA]:[ABVN]:[TFEMA]:[AP]:[HBA]:[mPEG] was 1:0.2:120:30:30:30. According to the ^{1}H NMR result (unpresented data), the enzymatic monomer transformation is efficient and the TFEMA has been found to combine with the alcohols to form monomers in 4 hours, consistent with our previous study.[39] In the current system all three functional alcohols including AP, HBA and mPEG were completely converted into corresponding monomers in ~ 4 h (data not presented). The kinetics study of the one-pot RAFT polymerization is shown in Fig. 1, and approximately 78% of the monomer has been polymerized after 24 h. During the course of polymerization, the $\ln([M]_0/[M])$ value increased linearly over time, indicating a pseudo-first-order kinetic plot (Fig. 1a) while the molecular weights of polymers also increased linearly versus monomer conversions, and all the polymers showed narrow polydispersity indices (PDIs < 1.3) (Fig. 1b) suggesting RAFT polymerization was well controlled despite the presence of enzymatic monomer transformation between TFEMA and functional alcohols.

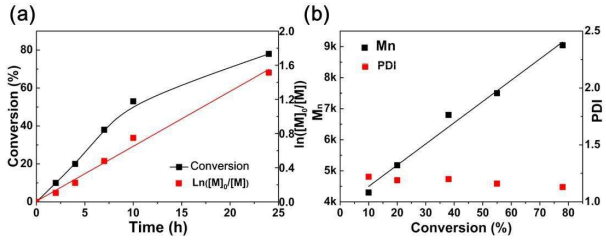

Fig. 1 One-pot synthesis of multifunctional copolymer (**Polymer 1**) via concurrent RAFT polymerization and enzymatic monomer transformation. (a) Monomer conversions and kinetics plot *versus* polymerization time; (b) molecular weights and PDIs *versus* monomer conversions. [CETPA]=12.5 mM; [ABVN]=2.6 mM; [TFEMA]$_0$=1.35 M; [AP]$_0$=0.33 M; [HBA]$_0$=0.33 M; [mPEG]$_0$=0.33 M; [TEA]=1.0 M; Novozym 435=0.5 g; toluene=6.0 mL; T=50 °C.

According to the UV analysis of the trithiocarbonate end group of the polymer, the molecular weight of obtained polymer was estimated to be ~ 15800 g/mol, similar to the theoretical value (17500 g/mol) calculated by conversion. The predesigned functional groups, including the benzaldehyde group (9.80, 7.82

and 7.05 ppm), the ester group of TFEMA (4.48 ppm), the methylene adjacent to the azido group (3.38 ppm) and the methoxy group of PEG chain end (3.18 ppm) can be clearly identified in the **Polymer 1** structure using ^{1}H NMR analysis (Fig. 2a), indicating the successful incorporation of those functional groups into the polymer. It is noted that the ratio of trifluoroethyl, azido, benzaldehyde and mPEG moieties in the polymer was calculated as 1:1.2:1:0.9 based on the integral of those functional groups, similar to the precursor alcohols ratio of 1:1:1:1, suggesting the composition of the final polymer can be readily regulated through the adjustment of initial feeding ratio of the functionalized alcohols and the acyl donor monomer TFEMA.

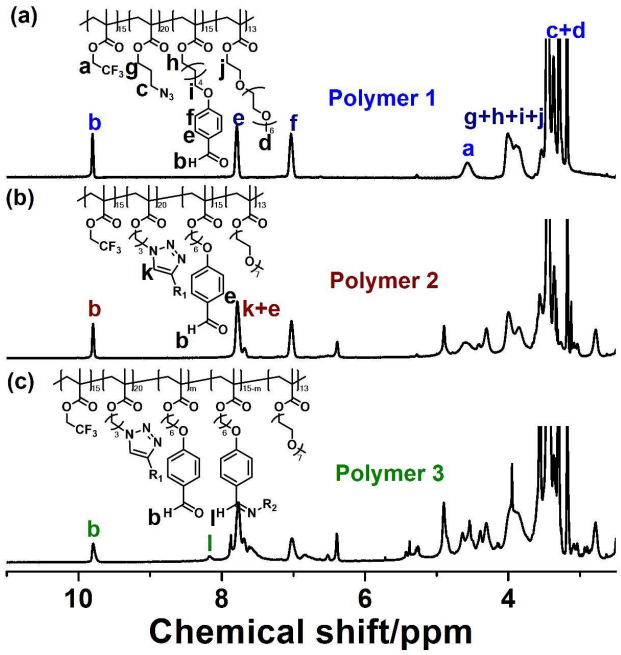

Fig. 2 The partial ^{1}H NMR spectra (DMSO-d6) of (a) multifunctional **Polymer 1** from concurrent RAFT-enzymatic polymerization system; (b) **Polymer 2** formed using a CuAAc click reaction between **Polymer 1** and alkyne modified glucosamine; (c) **Polymer 3** formed after conjugation of **Polymer 2** with dox.

Sugar moiety has been widely recognized as a possible targeting ligand for tumor treatment.[43-44] Thus, a glucose containing polymer (**Polymer 2**) was further prepared by conjugation between alkyne modified glucosamine and **Polymer 1** via a CuAAc click reaction using a mixed methanol/THF solution at room temperature for 24 h. As shown in Fig. 2b, the peak corresponding to the CH in triazole ring formed by click reaction can be seen at 7.82 ppm (overlapped by the proton on benzene ring). Meanwhile, IR spectra of the polymers revealed the characteristic azido adsorption peak (2100 cm^{-1} in **Polymer 1**) completely disappeared after click reaction while a peak corresponding to hydroxyl groups of glucosamine on **Polymer 2** appeared at 3290 cm^{-1} indicating the full conversion of the azido group (Fig. 3a). The GPC trace of **Polymer 2** exhibited a monomodal peak (PDI~1.32) and shifted to higher molecular weight region, confirming the successful introduction of glucosamine into **Polymer 1** (Fig. 3b).

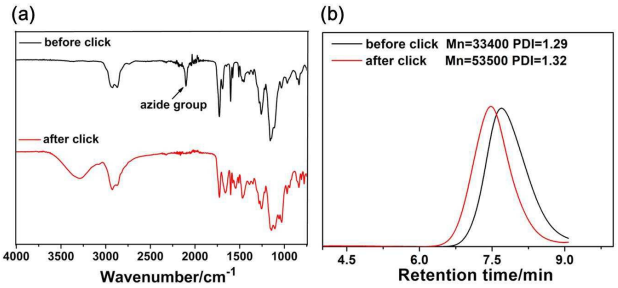

Fig. 3 (a) IR spectra of polymers before and after CuAAc click reaction; (b) GPC (DMF) traces of polymers before and after CuAAc click reaction.

Various drug carrier features of **Polymer 2** have been considered in detail including its cytotoxicity, imaging capability and protein recognition ability. The cytotoxicity of **Polymer 2** was first investigated via CCK-8 assay using HeLa cells. The HeLa cells were incubated with concentrations of **Polymer 2** ranging from 5-500 μg/mL for 24 h, then assessed for viability. As shown in Fig. 4, almost 100% cell viability was achieved even at the highest polymer concentration (500 μg/mL), indicating **Polymer 2** is not cytotoxic.

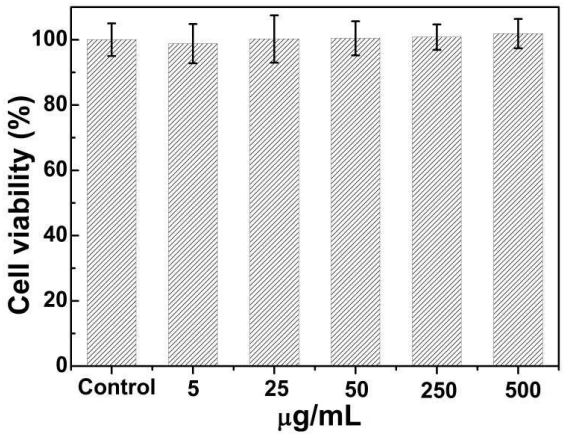

Fig. 4 Viability of HeLa cells after incubation with various concentrations of **Polymer 2** for 24 h. The cell viability in the absence of **Polymer 2** was set as control, n=3.

Polymer 2 was also evaluated for its potential as a ^{19}F MRI agent. A single peak at -72 ppm can be clearly observed on the ^{19}F NMR spectrum of **Polymer 2** (Fig. S1). The spin–lattice (T_1) and spin–spin (T_2) relaxations times of the **Polymer 2** were measured to be 380 ms and 30 ms, respectively. To show the imaging capabilities of the polymer, a ^{19}F phantom imaging study was conducted in a 400 MHz preclinical system and the results are shown in Fig 5. In the ^{1}H image of the phantom (Fig. 5a), two compartments containing 0.2 wt% Gd/DTPA in H_2O (area 1) and 10 mg/mL **Polymer 2** in H_2O (area 2) can be clearly identified. In the corresponding ^{19}F phantom image at ^{19}F frequency (Fig. 5b), only the ^{19}F signal coming from area 2 is present. This proof of principle experiment shows the potential of **Polymer 2** as a signal generating agent for ^{19}F MR imaging.

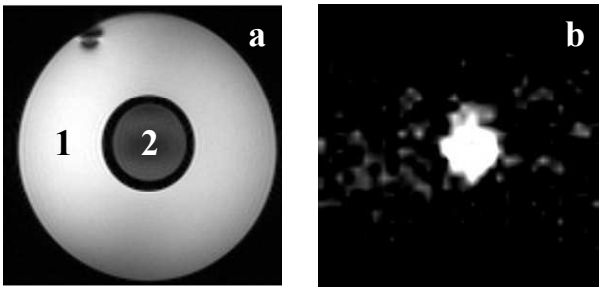

Fig. 5 (a) ^{1}H phantom image; (b) ^{19}F phantom image of **Polymer 2**. Area 1 contained 0.2 wt% Gd/DTPA in H_2O; area 2 contained 10 mg/mL **Polymer 2** in H_2O.

The turbidity test was operated to test the interaction between lectin (a highly specific sugar-binding protein) and **Polymer 2** (Fig. 6). When a **Polymer 2** solution (0.1 mL, 1.0 mg/mL in 10 mM PBS buffer, pH ~ 7.4) was mixed with lectin in solution (0.4 mL, 0.5 mg/mL in 10 mM PBS buffer, pH ~ 7.4), the turbidity of mixture was found to increase with time, indicating aggregation of the lectin in the presence of **Polymer 2**. Furthermore, when D-glucose aqueous solution (50 μL, 2 mg/mL) was added to the mixture the turbidity decreased immediately, confirming the increased turbidity comes from the affinity between the glucose groups on polymer and lectin. This lectin binding assay demonstrates the multi-sugar groups can be useful for recognition by the polymeric drug carrier of the target cells.

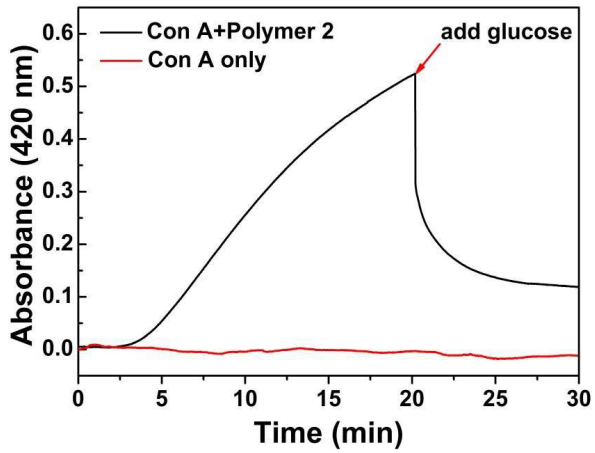

Fig. 6 Turbidity assay of **Polymer 2** with lectin association binding and dissociation competitive assay of after addition of D-glucose. (Absorbance at 420 nm was collected every 1 s for 20 min, then 50 μL of glucose aqueous solution (2.0 mg/mL) was added and the absorbance at 420 nm was recorded every 1 s for another 10 min).

These experiments demonstrate potential for **Polymer 2** as a possible multifunctional drug carrier. We then conjugated the anti-cancer drug dox to **Polymer 2** to form a polymer-dox complex (**Polymer 3**) via formation of an imine bond between the amine group of dox and the benzaldehyde moiety of **Polymer 2**. The reaction was performed in DMSO at 30 °C for 48 h. As shown in the ^{1}H NMR spectrum of **Polymer 3** (Fig. 2c), the peak corresponding to the CH of imine bond at 8.10 ppm could be clearly observed, and the molar conjugation efficiency of dox has been estimated to be 34% calculated using the integral ratio of remaining aldehyde group and imine group.

Polymer 3 is amphiphilic and can self-assemble into spherical micelles in aqueous solution. The micelle diameter has been analyzed as ~30 nm by TEM (Fig. 7a), and ~35 nm by DLS (Fig. 7b) which is within the optimal particle size range for drug delivery (10-100 nm) according to enhanced permeability and retention (EPR) effect.[45-47]

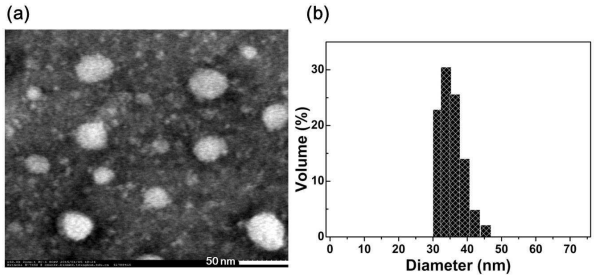

Fig. 7 (a) TEM image; (b) DLS measurement of micelles formed by **Polymer 3** (concentration of 0.5 mg/mL in aqueous solution).

Dox was conjugated to **Polymer 3** via the pH-sensitive imine bond which is unstable in acidic media. Thus we are able to study the release of dox from **Polymer 3** at different pH conditions (pH 7.4 and pH 5.5). As expected, at pH 5.5, dox was released significantly faster than at pH 7.4 due to the more rapid hydrolysis of the imine bond. About 78% of the conjugated dox was released after 36 h of incubation compared to only 40% released at pH 7.4 (Fig. 8). As tumors often exhibit lower pH microenvironments than normal cells,[48] this pH responsive property might enhance the release of dox when **Polymer 3** approaches the tumor diminishing its side effects and promoting drug efficacy.

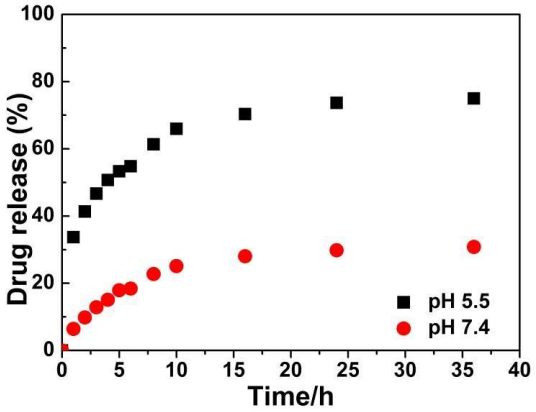

Fig. 8 Dox release at pH 5.5 and pH 7.4 at 37 °C.

The cytotoxic effects of free dox and **Polymer 3** against L929 cells (as the model for normal cells) and HeLa cells (as the model for tumor cells) were evaluated. We showed the viability of cells is dependent on the dox concentrations and cell types. **Polymer 3** demonstrated lower cytotoxicity against L929 cells than native dox (Fig. 9a). High concentrations of free dox showed significant toxicity against HeLa cells and the **Polymer 3** conjugated dox exhibited comparable *in vitro* cytotoxicity to native dox (Fig. 9b).

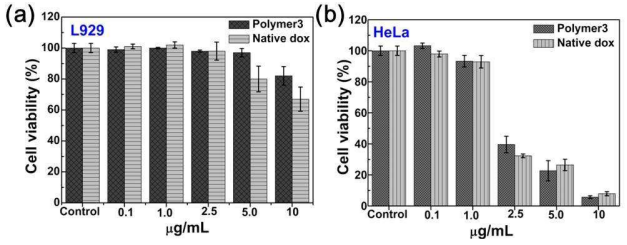

Fig. 9 Cytotoxicity of native dox and **Polymer 3** with different dox concentrations against (a) L929 and (b) HeLa cells after incubation for 24 h, the viability of untreated cells was chosen as the control, n=3.

The cellular uptake of **Polymer 3** by HeLa cells was also studied using confocal laser scanning microscopy (CLSM). HeLa cells were incubated with **Polymer 3** for 4 h then micrographed using confocal microscopy. As shown in Fig. 10, red fluorescence originating from dox mainly located in cells, indicating successful endocytosis of **Polymer 3** by HeLa cells. After 24 h incubation the morphology of HeLa cells greatly changed, suggesting the HeLa cells were efficiently killed by the conjugated dox.

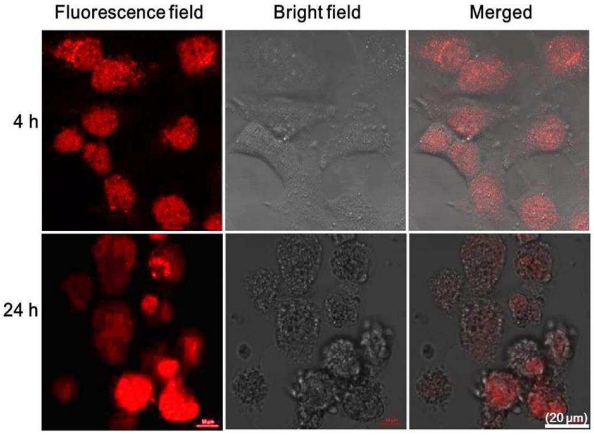

Fig. 10 CLSM images of HeLa cells treated with **Polymer 3** for (a) 4 h and (b) 24 h (dox concentration: 5 μg/mL).

Although more detailed research is still necessary to understand whether the drug carrier reduces the toxicity of drug to normal cells while retaining tumor potency stems from the targeting effect of glucose moiety, the easy endocytosis micelle structure or both, the cell viability results against L929 cell and HeLa cell preliminarily indicate therapeutic efficacy of multifunctional **Polymer 3** against tumor cells.

Conclusions

A CTP system has been employed to prepare copolymers possessing multiple functionalities. The enzymatic monomer transformation between acyl donor monomer TFEMA and multiple alcohols (AP, HBA and mPEG) efficiently generated new alcohol-based monomers which subsequently participated in RAFT polymerization to produce copolymers with pendant functional groups including azido, aldehyde and PEG groups. Polymerization kinetics exhibited a well-controlled RAFT process in the presence of enzymatic reaction and the obtained copolymer was further post-modified with glucosamine and dox via a CuAAc click reaction and imine chemistry to achieve a multifunctional theranostic agent. The fluorinated moiety makes the polymer a potential contrast agent for ^{19}F MR imaging. The binding assay between lectin and polymer carrier demonstrated its potential targeting effect. The polymer-dox conjugate could self-assemble in aqueous solution to form micelles which exhibited controlled release behavior of dox under different pH conditions. Normal cells were shown to be less susceptible than the cancer cells to both native and conjugated polymer-dox. The polymer-dox showed comparable cytotoxic effects to free dox against tumor cells. The current CTP system opens up an alternative method to synthesize multifunctional copolymers. Further work to further explore the application of this facile one-pot CTP system will be conducted in the future.

Acknowledgements

This research was supported by the National Science Foundation of China (21574073, 21134004, 21372033 and the QingLan Project). The authors thank David Beck for proof-reading the manuscript and Dr Ian Luck for helping with NMR.

Notes and references

[1]*The Key Laboratory of Bioorganic Phosphorus Chemistry & Chemical Biology (Ministry of Education), Department of Chemistry, Tsinghua University, Beijing 100084, China.*
[2]*Biomedical Resources Imaging Laboratory, Mark Wainwright Analytical Centre, The University of New South Wales, Sydney, NSW 2052, Australia.*
[3]*School of Chemistry, University of Sydney, Sydney, NSW 2006, Australia*
[4]*School of Petrochemical Engineering, Changzhou University, Changzhou, Jiangsu 213164, China.*
leitao@mail.tsinghua.edu.cn; hien.duong@sydney.edu.au; zhiming@cczu.edu.cn.

† Electronic Supplementary Information (ESI) available: Detailed experimental procedures, instruments and methods, functional alcohols synthesis and characterizations, polymerization and postmodification, F NMR spectrum etc. See DOI: 10.1039/b000000x/

(1) Lammers, T.; Aime, S.; Hennink, W. E.; Storm, G.; Kiessling, F. *Acc. Chem. Res.* **2011**, 44, 1029-1038.
(2) Chen, X.; Gambhir, S. S.; Cheon, J. *Acc. Chem. Res.* **2011**, 44, 841-841.
(3) Lee, D.-E.; Koo, H.; Sun, I.-C.; Ryu, J. H.; Kim, K.; Kwon, I. C. *Chem. Soc. Rev.* **2012**, 41, 2656-2672.
(4) Janib, S. M.; Moses, A. S.; MacKay, J. A. *Adv. Drug Deliv. Rev.* **2010**, 62, 1052-1063.
(5) Xie, J.; Lee, S.; Chen, X. *Adv. Drug Deliv. Rev.* **2010**, 62, 1064-1079.
(6) Choi, K. Y.; Liu, G.; Lee, S.; Chen, X. *Nanoscale* **2012**, 4, 330-342.
(7) Kelkar, S. S.; Reineke, T. M. *Bioconjugate Chem.* **2011**, 22, 1879-1903.
(8) Heo, D. N.; Yang, D. H.; Moon, H.-J.; Lee, J. B.; Bae, M. S.; Lee, S. C.; Lee, W. J.; Sun, I.-C.; Kwon, I. K. *Biomaterials* **2012**, 33, 856-866.
(9) Kennedy, L. C.; Bickford, L. R.; Lewinski, N. A.; Coughlin, A. J.; Hu, Y.; Day, E. S.; West, J. L.; Drezek, R. A. *Small* **2011**, 7, 169-183.
(10) Lee, J. E.; Lee, N.; Kim, T.; Kim, J.; Hyeon, T. *Acc. Chem. Res.* **2011**, 44, 893-902.
(11) Ambrogio, M. W.; Thomas, C. R.; Zhao, Y.-L.; Zink, J. I.; Stoddart, J. F. *Acc. Chem. Res.* **2011**, 44, 903-913.
(12) Ho, Y.-P.; Leong, K. W. *Nanoscale* **2010**, 2, 60-68.
(13) Tan, A.; Yildirimer, L.; Rajadas, J.; De La Peña, H.; Pastorin, G.; Seifalian, A. *Nanomedicine* **2011**, 6, 1101-1114.
(14) Santhosh, P. B.; Ulrih, N. P. *Cancer Lett.* **2013**, 336, 8-17.

(15) Sun, C.; Fang, C.; Stephen, Z.; Veiseh, O.; Hansen, S.; Lee, D.; Ellenbogen, R. G.; Olson, J.; Zhang, M. *Nanomedicine* **2008**, 3, 495-505.
(16) Santra, S.; Kaittanis, C.; Grimm, J.; Perez, J. M. *Small* **2009**, 5, 1862-1868.
(17) Singh, N.; Jenkins, G. J.; Asadi, R.; Doak, S. H. *Nano Rev.* **2010**, 1.
(18) Soenen, S. J.; Rivera-Gil, P.; Montenegro, J.-M.; Parak, W. J.; De Smedt, S. C.; Braeckmans, K. *Nano Today* **2011**, 6, 446-465.
(19) Fadeel, B.; Garcia-Bennett, A. E. *Adv. Drug Deliv. Rev.* **2010**, 62, 362-374.
(20) Krasia-Christoforou, T.; Georgiou, T. K. *J. Mater. Chem. B* **2013**, 1, 3002-3025.
(21) Luk, B. T.; Fang, R. H.; Zhang, L. *Theranostics* **2012**, 2, 1117-1126.
(22) Puri, A.; Blumenthal, R. *Acc. Chem. Res.* **2011**, 44, 1071-1079.
(23) Wang, Z.; Niu, G.; Chen, X. *Pharm. Res.* **2014**, 31, 1358-1376.
(24) Li, X.; Qian, Y.; Liu, T.; Hu, X.; Zhang, G.; You, Y.; Liu, S. *Biomaterials* **2011**, 32, 6595-6605.
(25) Liu, Y.; Feng, L.; Liu, T.; Zhang, L.; Yao, Y.; Yu, D.; Wang, L.; Zhang, N. *Nanoscale* **2014**, 6, 3231-3242.
(26) Hsu, C.-Y.; Nieh, M.-P.; Lai, P.-S. *Chem. Commun.* **2012**, 48, 9343-9345.
(27) Wang, S.; Kim, G.; Lee, Y.-E. K.; Hah, H. J.; Ethirajan, M.; Pandey, R. K.; Kopelman, R. *ACS nano* **2012**, 6, 6843-6851.
(28) Duncan, R. *Curr. Opin. Biotechnol.* **2011**, 22, 492-501.
(29) Nasongkla, N.; Bey, E.; Ren, J.; Ai, H.; Khemtong, C.; Guthi, J. S.; Chin, S.-F.; Sherry, A. D.; Boothman, D. A.; Gao, *J. Nano Lett.* **2006**, 6, 2427-2430.
(30) Oerlemans, C.; Bult, W.; Bos, M.; Storm, G.; Nijsen, J. F. W.; Hennink, W. E. *Pharm. Res.* **2010**, 27, 2569-2589.
(31) Li, Y.; Lin, T.-y.; Luo, Y.; Liu, Q.; Xiao, W.; Guo, W.; Lac, D.; Zhang, H.; Feng, C.; Wachsmann-Hogiu, S. *Nat. Commun.* **2014**, 5.
(32) Basuki, J. S.; Esser, L.; Duong, H. T.; Zhang, Q.; Wilson, P.; Whittaker, M. R.; Haddleton, D. M.; Boyer, C; Davis, T. P. *Chem. Sci.* **2014**,5, 715-726.
(33) Nakatani, K.; Terashima, T.; Sawamoto, M. *J. Am. Chem. Soc.* **2009**, 131, 13600-13601.
(34) Geng, J.; Lindqvist, J.; Mantovani, G.; Haddleton, D. M. *Angew. Chem. Int. Ed.* **2008**, 47, 4180-4183.
(35) Fu, C.; Tao, L.; Zhang, Y.; Li, S.; Wei, Y. *Chem. Commun.* **2012**, 48, 9062-9064.
(36) Zhu, C.; Yang, B.; Zhao, Y.; Fu, C.; Tao, L.; Wei, Y. *Polym. Chem.* **2013**, 4, 5395-5400.
(37) Zhang, Y.; Zhao, Y.; Yang, B.; Zhu, C.; Wei, Y.; Tao, L. *Polym. Chem.* **2014**, 5, 1857-1862.
(38) Tao, L.; Fu, C.; Wei, Y. *Polym. Int.* **2015**, 64, 705-712.
(39) Zhang, Y.; Fu, C.; Zhu, C.; Wang, S.; Tao, L.; Wei, Y. *Polym. Chem.* **2013**, 4, 466-469.
(40) Wang, S.; Fu, C.; Zhang, Y.; Tao, L.; Li, S.; Wei, Y. *ACS Macro Lett.* **2012**, 1, 1224-1227.
(41) Fu, C.; Zhu, C.; Wang, S.; Liu, H.; Zhang, Y.; Guo, H.; Tao, L.; Wei, Y. *Polym. Chem.* **2013**, 4, 264-267.
(42) Fu, C.; Yang, B.; Zhu, C.; Wang, S.; Zhang, Y.; Wei, Y.; Tao, L. *Polym. Chem.* **2013**, 4, 5720-5725.
(43) Spain, S. G.; Cameron, N. R. *Polym. Chem.* **2011**, 2, 60-68.
(44) Li, X; Chen, G. *Polym. Chem.* **2015**, 6, 1417-1430.
(45) Maeda, H.; Wu, J.; Sawa, T.; Matsumura, Y.; Hori, K. *J. Controlled Release* **2000**, 65, 271-284.
(46) Fang, J.; Nakamura, H.; Maeda, H. *Adv. Drug Deliv. Rev.* **2011**, 63, 136-151.
(47) Torchilin, V. *Adv. Drug Deliv. Rev.* **2011**, 63, 131-135.
(48) Vaupel, P. In Semin. Radiat. Oncol.; *Elsevier*: **2004**, 14, 198-206.

Table of content

Facile Synthesis of Multifunctional Copolymer via a Concurrent RAFT-Enzymatic System for Theranostic Applications

Changkui Fu, Andre Bongers, Ke Wang, Bin Yang, Yuan Zhao, Haibo Wu, Yen Wei, Hien T. T. Duong, Zhiming Wang, Lei Tao

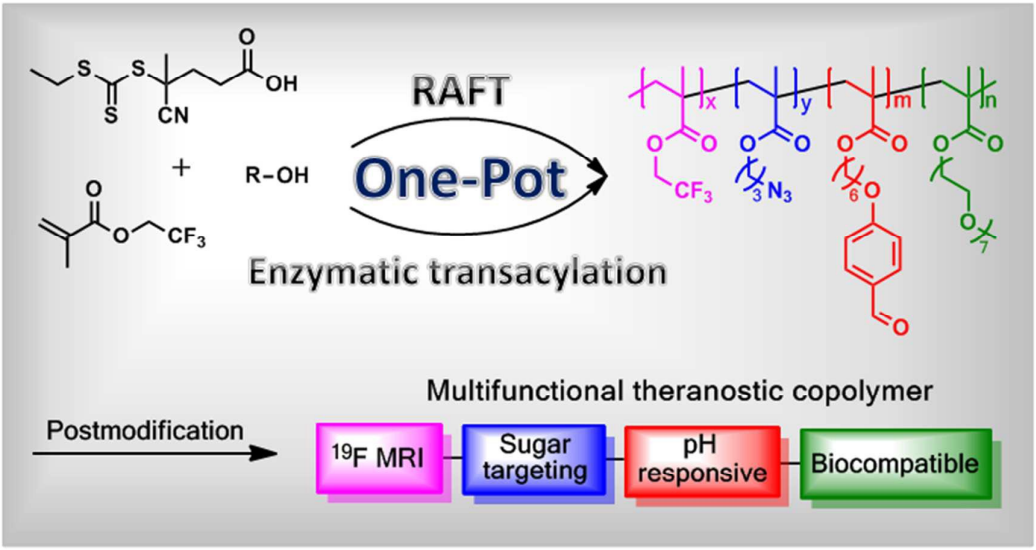

Through a straightforward concurrent RAFT-enzymatic multicomponent polymerization system and subsequent post-polymerization modifications, a multi-functional copolymer for theranostic application has been efficiently prepared.